Hexamerization of RepA from the *Escherichia coli* Plasmid pKL1†

Ján Burian,‡ Juan Ausió,§ Barry Phipps,|| Susan Moore,§ Douglas Dougan,|| and William Kay*,‡,§

Microtek International Ltd., 6761 Kirkpatrick Crescent, Saanichton, British Columbia, V8M 1Z8, Canada, Department of Biochemistry and Microbiology and the Canadian Bacterial Diseases Network, University of Victoria, Petch Building, P.O. Box 3055 Victoria, British Columbia, V8W 3P6 Canada, and Department of Biological Sciences, University of Calgary, Calgary, Alberta, T2N 1N4 Canada

Received February 28, 2003; Revised Manuscript Received June 25, 2003

ABSTRACT: The *Escherichia coli* plasmid pKL1 is one of the smallest bacterial plasmids. It encodes a single, autoregulating structural gene, *repA*, responsible for replication and copy number control. The oligomerization of RepA was previously proposed as the basis of a strategy for pKL1 copy number control. To elucidate the oligomerization properties of RepA in solution, RepA was expressed in *E. coli*; purified by ion exchange and hydrophobic chromatography; and examined in solution by spectrapolarimetry, light scattering, sedimentation velocity, and equilibrium ultracentrifugation. RepA behaved as a concentration-dependent equilibrium of dimers and hexamers. Conformational parameters of the RepA hexameric complex were determined. These results support the proposed autogenous regulatory model whereby RepA hexamers negatively regulate *repA* expression thereby affecting the copy number control of pKL1. RepA of pKL1 is the first plasmid replication initiation protein documented to be in dimeric−hexameric forms.

Plasmids are autonomous extrachromosomal DNA elements maintained at defined copy numbers in bacterial cells. Plasmids normally coordinate their replication rates with host cell growth to ensure their perpetuation. This is achieved via various autoregulatory control mechanism(s) whereby plasmid DNA concentration affects the plasmid replication rate (copy number control) and hence establishes plasmid copy number/cell.

The best understood circular plasmid replication and regulation system is that of the ColE1 plasmid family. It is based on the formation of a trans-acting antisense RNA,[1] which is complementary to a region at the 5′ end of the RNA preprimer; their pairing abolishes the maturation of the requisite replication primer. These plasmids characteristically depend on RNaseH and DNA polymerase I (PolA), which initially elongates a mature replication primer later to be replaced with DNA polymerase III. Some ColE1 replicons also encode an auxiliary protein regulator, Rom, to enhance the rate of formation of the inhibitory antisense RNA−preprimer RNA complex. Overall, this represents a rather relaxed version of plasmid copy number control resulting in tens to hundreds of plasmid copies per cell (*1*−*4*).

Other plasmids have developed more stringent, *polA*-independent control mechanisms. These generally involve a specific plasmid-encoded replication protein, Rep, necessary for the initiation of plasmid replication. The rate of synthesis of Rep can be controlled at the transcriptional and/or translational levels by antisense RNA and/or a repressor. For example, the expression of *repA* of plasmid R1 is controlled by antisense RNA at the translational level and by an auxiliary protein repressor, CopB, at the transcriptional level (*5*−*10*). Several plasmids even invoke a dual regulation strategy for Rep expression involving antisense RNA as well as a transcriptional repressor to fine-tune the maintenance of copy number. Both elements sense and correct the fluctuation in copy number and together constitute a more stringent degree of regulation than exhibited by either element alone (*11*−*14*).

Particularly large plasmids often employ plasmid-specific iterons, DNA arrays comprised of ∼20 bp repeats, to bind associated Rep proteins responsible for both initiation and control of replication. Iterons effectively allow the Rep-mediated coupling of plasmid replication origins (handcuffing) that prevents plasmid over-replication (*15*).

At the lower end of the plasmid size spectrum the unusually small (1.549 kb), cryptic plasmid, pKL1 (Genbank U81610) (*16*), seems to employ a different mechanism of autoregulatory plasmid control independent of iterons and/or antisense RNA (*17*). This mechanism may be a general copy number control model especially for small, IHF-dependent plasmids (*17*−*19*). The present work documents a structural study of purified pKL1 RepA and its reversible, concentration-dependent hexamerization in solution. The

† The research was funded by Microtek International (1998) Ltd. (J.B.), the National Sciences and Engineering Research Council of Canada and the Canadian Bacterial Diseases Network−Centre of Excellence (CBDN) by grants to W.K., and a research grant from the Natural Sciences and Engineering Research Council of Canada to B.P. B.P. also holds a Medical Scholar Award from the Alberta Heritage Foundation for Medical Research.

* Corresponding author. Tel: (250) 721-7078. Fax: (250) 721-8882. E-mail: wkay@uvic.ca.

‡ Microtek International Ltd.

§ University of Victoria.

|| University of Calgary.

[1] Abbreviations: *cop*, copy number control; DNA, deoxyribonucleic acid; DTT, dithiothreitol; EDTA, ethylenediaminetetraacetic acid; IHF, integration host factor; *inc*, incompatibility; DLS, dynamic light scattering; SLS, static light scattering; M_r, relative molecular weight; NA, nucleic acid; PAGE, polyacrylamide gel electrophoresis; Rep, plasmid replication protein; RNA, ribonucleic acid; SDS, sodium dodecylsulphate.

10.1021/bi034341b CCC: $25.00
Published on Web 08/01/2003

results support and refine the proposed model for pKL1 copy number control.

MATERIALS AND METHODS

Expression and Purification of RepA. RepA was purified from 3 L of *Escherichia coli* BL21 (F^- *ompT lon hsdS*$_B$ $r_B^-m_B^-$) that contained plasmids pBGL-R (*17*) and pGP1-2 (*20*). The culture in six 4-L Erlenmeyer flasks containing 500 mL of TFB (*21*) was vigorously shaken at 28 °C overnight. An equal volume of fresh medium was added, and incubation was continued at 42 °C for 2 h. Cells were harvested by centrifugation, washed with 50 mmol L^{-1} Tris-HCl, 0.2 mol L^{-1} NaCl, 1 mmol L^{-1} EDTA, pH 7.6 and resuspended in 250 mL of the same buffer. Cells were broken in a French Press Homogenizer at 10 000 psi, the homogenate was cleared by centrifugation first at 15 000*g* and subsequently at 30 000*g*, and the RepA-containing fractions precipitated with 7.3% poly(ethylene glycol) 8000 (Sigma). The precipitate was centrifuged at 15 000*g*, resuspended in 100 mL of 50 mmol L^{-1} Tris-HCl, 100 mmol L^{-1} NaCl, 1 mmol L^{-1} EDTA, pH 7.6 and loaded onto a 200-mL DEAE cellulose column (Whatman). After rigorous washing with the loading buffer, RepA was eluted with a linear 0.2−1 M gradient of NaCl in one major peak. Fractions from the peak were analyzed by SDS−PAGE, pooled based on the purity of RepA-containing fractions, and stored on ice. The concentration of NaCl was slowly increased to 4 M in the pooled fractions and then loaded onto a 50-mL Phenyl Sepharose (Pharmacia) hydrophobic interaction column (HIC). After thorough washing with a buffer comprised of 50 mmol L^{-1} Tris-HCl, 4 mmol L^{-1} NaCl, 1 mmol L^{-1} EDTA, pH 7.6, RepA was eluted again in one major peak using a descending 4.0−0.5 M NaCl gradient in 50 mmol L^{-1} Tris-HCl and 1 mmol L^{-1} EDTA, pH 7.6. Fractions from the peak were once again analyzed by SDS−PAGE, pooled based on RepA purity and stored on ice for the duration of all experiments.

Samples used for light scattering studies were alternatively further purified by affinity column chromatography on 200-mL Heparin-Sepharose (Pharmacia). The protein was loaded onto the column in 10 mmol L^{-1} Tris-HCl pH 7.6, 1 mmol L^{-1} EDTA, 0.5 M KCl (TE/0.5 M KCl), washed with two bed volumes of the same buffer, and eluted with TE/2 M KCl. RepA-containing fractions were pooled and dialyzed against TE/0.5 M KCl.

Analytical Ultracentrifugation. Sedimentation velocity and sedimentation equilibrium experiments were carried out using a Beckman XL-A analytical ultracentrifuge using An-55 AL 9 (aluminum) and An-60 Ti (titanium) rotors, respectively. The samples were loaded into double sector Kel-F 12 mm double sector cells. Temperature and speed conditions are indicated in the figure legends. Sedimentation velocity scans were analyzed using XL-A Ultra Scan version 4.1 sedimentation data analysis software (Borries Demeler, Missoula, MT), which employs a published method of boundary analysis (*22*). Sedimentation equilibrium scans were analyzed using a nonlinear, least squares, curve fitting algorithm (*23*) contained in the XL-A data software analysis.

Conformational Parameters. By combining sedimentation equilibrium and sedimentation velocity results, it was possible to determine the conformational parameters of RepA in its hexameric form. The frictional coefficients and asymmetry of the complex were calculated as described previously (*24*) assuming a prolate ellipsoid shape of semiaxes a and b (γ = b/a) with

$$f/f_o = \frac{(1-\gamma^2)^{1/2}}{\gamma^{2/3}\ln\dfrac{1+(1-\gamma^2)^{1/2}}{\gamma}}$$

where $f = M/sN\ (1 - \bar{\nu}\rho) = 6\pi\eta R_s$, $f_o = 6\pi\eta R_o$, $R_o = [3M(\bar{\nu} + \epsilon_1)/4\pi N]^{1/3}$ and M = the relative MW of the complex, s = the sedimentation coefficient, N = Avogadro's number, $\bar{\nu}$ = the partial specific volume, ρ = solution density, η = viscosity of the solvent, $R_s = (f/f_o)$, R_o = Stokes radius, R_o = the radius of the sphere corresponding to the volume of the macromolecule, and ϵ_1 = preferential hydration parameter (*25*). A value of $\epsilon_1 = 0.22$ g of H_2O/g of protein was used in the calculations (*26*). The ratio $f/f_o = 1$ for a perfectly spherical molecule and higher values are indicative of the extent of departure from the spherical shape. From γ, the values for the semiaxes a and b were determined for a hydrated volume V_h of the protein equivalent to a prolate ellipsoid $V_h = M/sN\ (\bar{\nu} + \epsilon_1) = (4/3)\pi ab^2$. The radius of gyration can then be calculated from equation $R_G = a\sqrt{(2+\gamma^2)/5}$ (*27*). The partial specific volume of the protein (0.737 $cm^3\ g^{-1}$) was calculated from its amino acid composition (*28*). The extinction coefficient of the protein at 280 nm (ϵ = 22 430) was determined from protein sequence information as described by ref *29*.

Light Scattering. Dynamic light scattering (DLS) analysis was performed using a DynaPro MS/MSTC molecular sizing instrument (Protein Solutions), which measures the scattering of laser light of wavelength 827.6 nm by a protein sample, at a scattering angle of 90°. Samples (50 μL) of 150−480 μmol L^{-1} RepA in TE /0.5 mol L^{-1} KCl were passed through a 0.02 μm Whatman anodisc filter to remove particulate matter and placed in the instrument in a quartz cuvette. Approximately 100 measurements were collected for each sample, at 20 °C. Fluctuations in the intensity of scattered light were analyzed with Dynamics and DynaLS software to determine the translational diffusion coefficient D_T and consequently, the hydrodynamic radius R_H for each species of a distinct molecular size in the solution. The approximate M_r corresponding to a given R_H was obtained from a standard curve compiled from known R_H and M_r values of a large set of globular proteins.

Static light scattering (SLS) analysis was carried out using a mini-DAWN multi-angle light scattering (MALS) detector (Wyatt Technology Corp.) in chromatography mode, a technique known as SEC-MALS (size-exclusion chromatography-multi-angle light scattering). The MALS detector was connected to the outlet of an Agilent 1100 HPLC fitted with a Shodex KW 803 size-exclusion column. An Optilab DSP refractometer (Wyatt Technology Corp.) operating at 690 nm and an Agilent UV absorbance detector operating at 280 nm were placed immediately downstream of the MALS detector. For each experimental run, a 50-μL sample of RepA (5.6−310 μmol L^{-1}) in TE/0.5 mol L^{-1} KCl was injected onto the size-exclusion column and eluted with the same buffer at a flow rate of 0.5 mL min^{-1}. The HPLC column fractionated the protein sample according to size;

the MALS detector illuminated the eluted protein with laser light of wavelength 690 nm and measured the intensity of scattered light at three different angles. The shape-independent relative MW of the protein in each elution slice (0.5 s) was determined with Astra software, utilizing the light scattering signal extrapolated to zero scattering angle and the protein concentration obtained from the refractometer. A specific refractive index increment (d*n*/d*c*) value of 0.18 mL g^{-1} was used.

RESULTS

Purification of RepA. RepA was isolated from a 3 L culture of *E. coli* BL21 containing a temperature-inducible, phage T7 expression system (*17*). The relative purity of RepA after DEAE cellulose and Phenyl Sepharose column chromatography was reproducibly >95%.

RepA Concentration-Dependent Sedimentation. Analysis of 45 μmol L^{-1} RepA in the presence of 0.3 or 0.5 mol L^{-1} NaCl and 120 μmol L^{-1} RepA (0.5 mol L^{-1} NaCl) provided virtually identical results (Figure 1a). The sedimentation velocity showed that RepA formed a homogeneous complex sedimenting at 6.0 S. When the concentration of RepA was decreased to 5 μmol L^{-1}, the complex began to dissociate giving rise to a broad spectrum of components with smaller sedimentation coefficients (Figure 1b). However, this RepA complex was readily dissociated in the presence of 0.1% SDS (Figure 1c).

Subunit Composition of RepA by Sedimentation Equilibrium. The subunit composition of RepA oligomers was determined by sedimentation equilibrium (Figure 2). The concentration dependence of M_r across the cell at equilibrium at different rotor speeds is shown in Figure 2a. The lowest M_r observed (~40 000) corresponded approximately to RepA dimers. Figure 2b shows the best fit analysis for the gradient at equilibrium at 8000 rpm at a starting concentration corresponding to $A_{280} = 0.6$ (~27 μmol L^{-1}) using an ideal single component system as a model. The M_r (122 400) obtained in this way agrees well with the average value observed for RepA concentration dependence shown in Figure 2a under the same experimental conditions. The distribution of the residuals from this fit shows a slight trend that suggests the presence of a two-component system (Figure 2c). However, all attempts to analyze the data by fitting it to a two component or a multicomponent system failed to produce better fitting results. When the M_r averages obtained from fitting the equilibrium curve obtained at different starting protein concentrations at 8000 rpm were extrapolated to zero sample concentration, a value of M_r (103 500) was obtained, consistent with a hexameric complex of nominal MW, 107 758.

Conformational Parameters of RepA. The impossibility of determining the sedimentation coefficient of the RepA monomer precluded the construction of a model for the hexameric complex. Nevertheless, the hydrodynamic data available for the complex allowed the determination of its conformational parameters. Results of such analyses are shown in Table 1.

Dynamic Light Scattering. The molecular size dispersity of RepA was examined using DLS. A single, narrow peak was observed, indicating that the protein is indeed monodisperse (result not shown). From the translational diffusion coefficient, the hydrodynamic radius (R_H) of the molecular species was calculated to be 4.9 nm. Essentially identical results were obtained from a large number of independent trials over a concentration range of 150−480 μmol L^{-1}. An R_H of 4.9 nm corresponds to a M_r of 137 000 based on a standard curve comprised of globular proteins. This value is model-dependent; it does not take into account deviations of RepA from the average spherical shape of the test set of globular proteins.

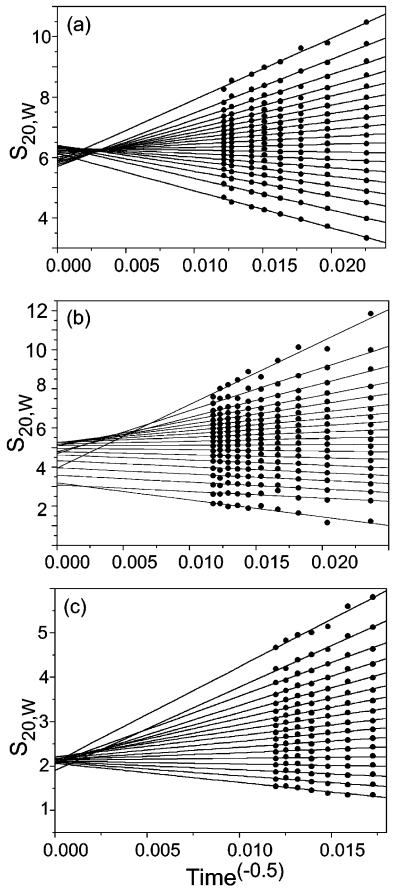

FIGURE 1: Sedimentation velocity analysis of RepA at different protein and NaCl concentrations and in the presence of SDS. (a) 45 μmol L^{-1} RepA in the presence of 0.3 mol L^{-1} NaCl, (b) 5 μmol L^{-1} RepA in the presence of 0.5 mol L^{-1} NaCl, and (c) 45 μmol L^{-1} RepA in the presence of 0.3 mol L^{-1} NaCl and 0.1% SDS. The buffer was 20 mmol L^{-1} Tris-HCl (pH 7.6), 1 mmol L^{-1} EDTA, and 0.1 mmol L^{-1} DTT. All runs were carried out at 44 000 rpm at 20 °C. Scans were analyzed according to the method of ref *22*, and the corresponding apparent sedimentation coefficients were extrapolated in a global linear fit to infinite time (zero on the inverse scale), where the intercepts mark the diffusion corrected *s* values. In the fan plots shown in this figure, the number of lines converging to a common $s_{20,W}$ is proportional to the fraction of sample sedimenting with this $s_{20,W}$ value. Results from experiment (a and c) show that this sample was quite homogeneous in composition and sedimented with *s* values around 6.0 S and ~2.1 S, respectively. Results from experiment (b) show that this sample was heterogeneous in composition and sedimented with *s* values from 3 to 4.5 S.

Static Light Scattering. A model-independent relative MW determination was carried out by means of static light scattering (SLS). RepA was fractionated on a size-exclusion column, and SLS measurements were made on the eluted protein species. The SLS signal at 90° was recorded as a function of elution time (results not shown). When a high concentration of RepA (310 μmol L^{-1}) was applied to the

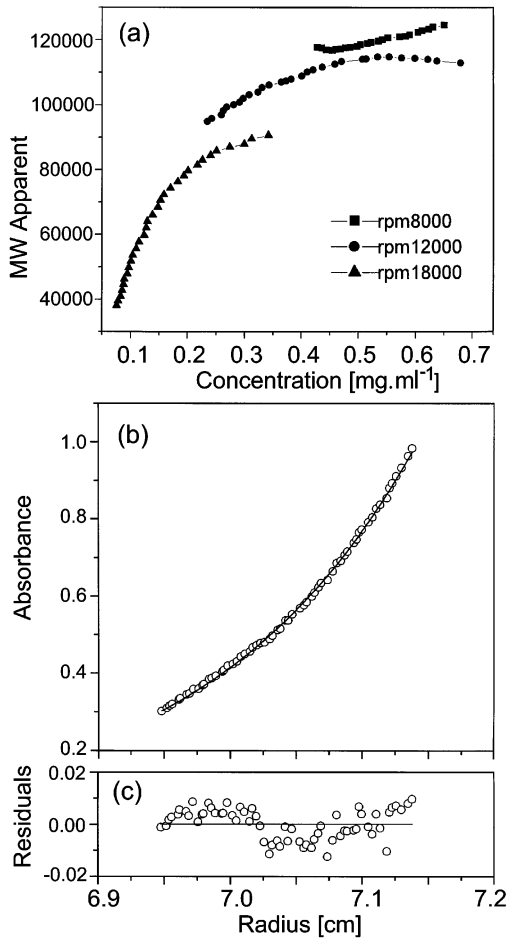

FIGURE 2: Sedimentation equilibrium analysis of RepA. (a) Relative MW concentration dependence analysis at rotor speeds 8000, 12 000, and 18 000 rpm at 20 °C. Buffer composition: 0.5 mol L^{-1} NaCl, 20 mmol L^{-1} Tris-HCl (pH 7.6), 0.1 mmol L^{-1} DTT, 1 mmol L^{-1} EDTA buffer. (b) The continuous line indicates the fitting to a single ideal species of M_r 122 400. The A_{280} of the starting sample was 0.6, and the analysis shown corresponds to the data collected at the equilibrium at 8000 rpm. (C) χ^2 residuals as a function of the radial distance for the best fit (solid line in b) to the experimental data (open circles in b) (*41*).

Table 1: Conformational Parameters of the RepA Hexameric Complex

relative MW[a]	107758
$\bar{v}$ (cm^3/g)	0.737
$s_{20,w}$ (S)	6.0
f/f_o	1.21
R_o (nm)	3.44
R_s (nm)	4.06
a/b	4.40
a (nm)	9.24
b (nm)	2.10
R_G (nm)	5.93

[a] The M_r of the hexamer was calculated from the M_r of the monomer as deduced from the amino acid sequence (M_r = 17 959.6 for the Rep A monomer); $\bar{v}$—density; $s_{20,w}$—sedimentation coefficient corrected to water at 20 °C; f/f_o—frictional ratio; R_o—radius of a sphere corresponding to a macromolecule; R_s—Stokes radius. a and b are the values for the semiaxes determined for a hydrated volume V_h of the protein equivalent to a prolate ellipsoid. R_G—radius of gyration.

column, a large narrow peak was observed. This peak was an equivalent to the peak observed by DLS, as judged by similar hydrodynamic radii. The smaller peak eluting earlier constituted large aggregates of $M_r > 1 \times 10^7$ although only

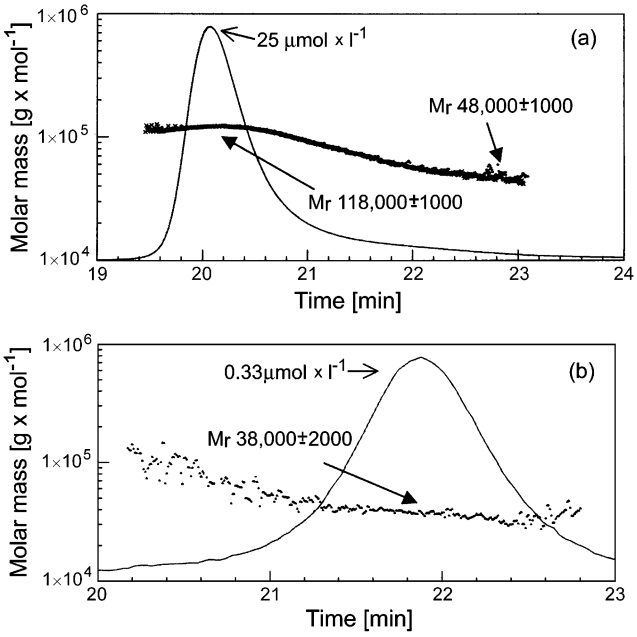

FIGURE 3: Model-independent relative MW of RepA determined by SEC-MALS. (a) M_r plotted as a function of elution time superimposed on the refractive index chromatogram for RepA applied at 310 μmol L^{-1}. Results from two independent injections are plotted. The highest eluted concentration of RepA and relative MW values (M_r) at indicated points are shown. (b) Similar plot for RepA applied at 5.6 μmol L^{-1} (one injection).

present in trace amounts. The intensity of scattered light was proportional to both M_r and concentration; hence, the light scattering signal was greatly enhanced for these aggregates. No corresponding signal was seen on the refractometer or the UV detector (results not shown), indicating that very little aggregate was present in the sample. A plot of M_r versus elution time (Figure 3a) for the large peak yielded a M_r (118 000 ± 1000) for RepA, suggesting that the protein is either a hexamer or a heptamer. The concentration of the protein at the highest point in this peak was determined by the refractometer signal to be 25 μmol L^{-1}. When a much lower concentration of sample (5.6 μmol L^{-1}) was applied, the highest concentration of eluted RepA was 0.33 μmol L^{-1}, and the M_r was 38 000 ± 2000 M_r, indicative of a dimer (Figure 3b). At an intermediate concentration (28 μmol L^{-1} applied, 1.2 μmol L^{-1} eluted), a broad, skewed peak was observed that suggested the presence of both oligomer and dimer (data not shown). Comparison of protein concentrations determined by refractometry with UV absorbance signals gave a molar extinction coefficient for RepA of ϵ_{280} = 21 900 M^{-1} cm^{-1}. The molar extinction coefficient calculated from the RepA protein sequence was ϵ_{280} = 22 430 ± 5% M^{-1} cm^{-1}.

DISCUSSION

Replication control of the *E. coli* plasmid pKL1 is based on specific DNA−protein interactions at the *cop* locus involving RepA and IHF proteins. These interactions were recently studied by gel retardation, DNase I footprinting, and cross-linked oligomeric RepA, Southwestern blots (*17*). The results showed that RepA interacts with plasmid pKL1 DNA as either a monomer or dimer and as an oligomer at two distinct binding sites (BD1 and BD2). However, the exact nature of the RepA oligomers remained unresolved yet

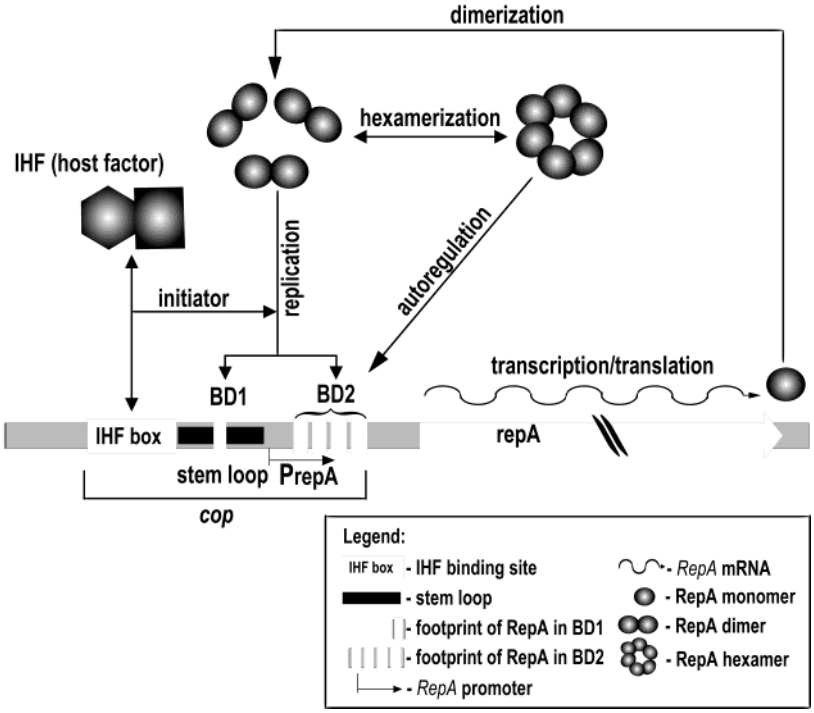

FIGURE 4: Regulation of replication of plasmid pKL1. The pKL1 copy number control (*cop*) region comprises an incompatibility (*inc*) determinant including the *repA* promoter, two RepA binding domains (BD1 and BD2), and an IHF box. RepA-DNA binding and DNase I protection assays revealed the affinity of RepA dimers and hexamers to binding sites BD1 and BD2 (*17*). DNA protection at BD1 corresponds to binding of a RepA dimer, whereas an iterative protection pattern at BD2 in the *repA* promoter region suggested a more complex binding of RepA hexamers. Both binding sites (BD1 and BD2) were shown to be necessary for replication (*17*). The major factor in copy number control is autoregulation of the *repA* gene by RepA hexamers, which sets the concentration of RepA dimers available for initiation of plasmid replication (*17*). Host factor IHF likely facilitates binding of RepA dimers to BD1 in vivo, which leads to initiation of replication. Gel retardation assays showed that RepA releases IHF from its binding domain. RepA binding to BD1 and BD2 is regarded as the initiating step in plasmid replication when a cruciform stem loop structure is formed (*17*). As RepA concentration increases, dimers form hexamers with an affinity for BD2, autoregulating transcription of *repA*. The concentration of RepA hexamers and dimers determines plasmid copy number. There is an approximate correlation of RepA expression in trans with plasmid copy number that could be modulated within a fairly wide range (*17*). In RepA overproducing conditions (RepA produced in trans from a helper plasmid), hexamers are formed, but the absolute concentration of dimers is also increased, and it is quite possible that the dimers still bind to BD1, and RepA continues to facilitate replication without IHF assistance (*17*). It is presumed that the function of RepA dimers is only in the initiation of replication, and the natural function of hexamers is the autoregulation of *repA* expression and not the initiation of replication; otherwise, it would provide a degenerate system for plasmid DNA replication.

crucially important when considering the precise nature of specific RepA−DNA interactions. To resolve this question, RepA structure in solution was studied by analytical ultracentrifugation and light scattering.

Preliminary sedimentation velocity results with DEAE-cellulose purified RepA showed the RepA complex to be unusually large and stable but readily aggregated in low salt solutions. UV spectra revealed a high content of nucleic acids (result not shown). When hydrophobic interaction chromatography (HIC) eliminated the nucleic acid content, RepA no longer aggregated in low salt solutions (Figure 1a) and was fully dissociated in the presence of 0.1% SDS to the monomeric form (Figure 1c). Because of the presence of SDS, no further attempt was made to determine any hydrodynamic parameters under these conditions; SDS was used only to fully dissociate RepA dimers and reveal RepA monomers.

The sedimentation coefficient of the RepA complex (6.0 S) is peculiarly large for a molecule with a relative MW equivalent to that of the RepA monomer or dimer as determined from its predicted amino acid sequence and suggests that the protein exists as a well-defined multisubunit complex (Figure 1a). It is important to emphasize that the fan plots from the sedimentation velocity analysis (*22*) consistently showed a crossover before infinite time. This indicates a marked dependence of the sedimentation coefficient on sample concentration (*30*). When the concentration of RepA was decreased to 5 μmol L^{-1}, the 6.0 S complex began to dissociate (Figure 1b). The sedimentation coefficient of the smaller component could not be accurately established as the sample could not be analyzed at the very low concentrations required for major complex dissociation. However, sedimentation equilibrium could be used to determine the subunit composition of the RepA complex (Figure 2). The results of analytical ultracentrifugation indicate that at low concentrations RepA is predominantly a stable dimer and at high concentrations predominantly a hexamer.

DLS and SLS experiments also showed RepA to be present as a distinct oligomeric form at moderate to high protein concentrations (Figure 3a). When low concentrations of RepA were analyzed by SLS, the results clearly indicated the predominance of dimers (Figure 3b). The hydrodynamic radius found by DLS indicated a larger than expected molecular weight for a hexamer, based on the assumption that the oligomer is shaped like an average globular protein. From the ratio of the measured hydrodynamic radius (4.9 nm) to the radius of a hydrated perfect sphere of the same

MW, the frictional ratio of the oligomer could be calculated to be 1.3−1.4, assuming RepA is either a hexamer or heptamer. Most globular proteins have frictional ratios between 1.1 and 1.2, indicating significant asymmetry in the shape of the RepA oligomer. The values for the Stokes radius and the radius of gyration of the 6.0 S complex calculated from sedimentation velocity were found to be in quite good agreement with the hydrodynamic radius of calculated from the light scattering results (Table 1). SLS also indicated that the RepA oligomer is either a hexamer or possibly a heptamer. The presence of some tailing toward a lower MW in the light scattering peak, even at very high RepA concentration, suggested that the main species may be in equilibrium with a small amount of a species of lower mass. A mixture of these species in the main peak would reduce the effective MW since this technique yields a value that is averaged over all molecules present suggesting the possible presence of a heptameric form.

Figure 4 summarizes previous (*17*) and current experimental evidence concerning pKL1 replication and proposes a refined model for the plasmid copy number control. Dimers of Rep proteins have been described for several plasmids, such as P1, F, R6K, and pSC101 (*31*−*33*). In the case of pSC101, its form of RepA was shown to be present as both monomers and dimers; RepA monomers bind to direct repeat iterons near the replication origin whereas dimers bind to a separate site thereby autoregulating RepA synthesis. This equilibrium between monomeric and dimeric forms of RepA has a key role in determining its effect on the replication of pSC101 (*34*). However, there are only two examples of hexameric proteins encoded by plasmids and somehow linked to plasmid replication: a helicase of the broad host range plasmid RSF1010 (*35*) and a hexamer−DNA complex reported for ArgR, which in addition to its role in host arginine metabolism, functions as an accessory factor in the resolution of plasmid ColE1 multimers by intramolecular recombination (*36*, *37*). In general, hexameric ring-shaped structures are not unusual for proteins involved in nucleic acid metabolism. For example, in *E. coli* DnaB, RuvB, and Rho proteins, all form hexameric ring-like structures (*38*−*40*). A hexameric ring-shaped structure might simply be required to encircle the target DNA site, making use of the topological linkage to prolong its residence on the DNA. RepA of pKL1 is the first plasmid replication initiation/autoregulatory protein documented to be in dimer−hexamer forms.

ACKNOWLEDGMENT

The authors would like to thank Dr. Michelle Chen (Wyatt Technology Corp.) for performing the static light scattering measurements.

REFERENCES

1. Goss, P. J., and Peccoud, J. (1999) *Pac. Symp. Biocomput.* 65−76.
2. Tomizawa, J., and Som, T. (1984) *Cell 38*, 871−8.
3. Tomizawa, J. (1990) *J. Mol. Biol. 212*, 695−708.
4. Tomizawa, J. (1990) *J. Mol. Biol. 212*, 683−94.
5. Blomberg, P., Nordström, K., and Wagner, E. G. (1992) *EMBO J. 11*, 2675−83.
6. Nordström, K., and Wagner, E. G. (1994) *Trends Biochem. Sci. 19*, 294−300.
7. Persson, C., Wagner, E. G., and Nordström, K. (1990) *EMBO J. 9*, 3777−85.
8. Persson, C., Wagner, E. G., and Nordström, K. (1990) *EMBO J. 9*, 3767−75.
9. Blomberg, P., Wagner, E. G., and Nordström, K. (1990) *EMBO J. 9*, 2331−40.
10. Soderbom, F., Binnie, U., Masters, M., and Wagner, E. G. (1997) *Mol. Microbiol. 26*, 493−504.
11. del Solar, G., Acebo, P., and Espinosa, M. (1995) *Mol. Microbiol. 18*, 913−24.
12. Brantl, S., and Wagner, E. G. (1997) *J. Bacteriol. 179*, 7016−24.
13. Brantl, S. (1994) *Mol. Microbiol. 14*, 473−83.
14. del Solar, G., Acebo, P., and Espinosa, M. (1997) *Mol. Microbiol. 23*, 95−108.
15. Chattoraj, D. K. (2000) *Mol. Microbiol. 37*, 467−76.
16. Burian, J., Guller, L., Mačor, M., and Kay, W. W. (1997) *Plasmid 37*, 2−14.
17. Burian, J., Stuchlík, S., and Kay, W. W. (1999) *J. Mol. Biol. 294*, 49−65.
18. del Solar, G., and Espinosa, M. (2000) *Mol. Microbiol. 37*, 492−500.
19. Bingle, L. E., and Thomas, C. M. (2001) *Curr. Opin. Microbiol. 4*, 194−200.
20. Tabor, S., and Richardson, C. C. (1985) *Proc. Natl. Acad. Sci. U.S.A. 82*, 1074−8.
21. Maniatis, T., Fritsch, E. E., and Sambrook, J. (1989) *Molecular cloning. A laboratory manual, 2nd ed.*, Cold Spring Harbor Laboratory Press, Cold Spring Harbor, Woodbury, New York.
22. Van Holde, K. E., and Weischet, W. O. (1978) *Biopolymers 17*, 1387−1401.
23. Johnson, M. L., Correia, J. J., Yphantis, D. A., and Halvorson, H. R. (1981) *Biophys. J. 36*, 575−88.
24. Ausió, J., Malencik, D. A., and Anderson, S. R. (1992) *Biophys. J. 61*, 1656−63.
25. Tanford, C. (1961) *The Physical Chemistry of Macromolecules*, John Wiley and Sons, New York.
26. Eisenberg, H. (1990) *Eur. J. Biochem. 187*, 7−22.
27. Haschemeyer, R., and Haschemeyer, A. (1973) *Proteins*, John Wiley and Sons, New York.
28. Perkins, S. J. (1986) *Eur. J. Biochem. 157*, 169−80.
29. Gill, S. C., and von Hippel, P. H. (1989) *Anal. Biochem. 182*, 319−26.
30. Demeler, B., Saber, H., and Hansen, J. C. (1997) *Biophys. J. 72*, 397−407.
31. Swack, J., Pal, S. K., Mason, R. J., Abeles, A. L., and Chattoraj, D. K. (1987) *J. Bacteriol. 169*, 3737−42.
32. Filutowitz, M., McEachern, M. J., and Helinski, D. R. (1986) *Proc. Natl. Acad. Sci. U.S.A. 83*, 9645−9.
33. Manen, D., and Caro, L. (1991) *Mol. Microbiol. 5*, 233−7.
34. Ingmer, H., Fong, E. L., and Cohen, S. N. (1995) *J. Mol. Biol. 250*, 309−14.
35. Scherzinger, M., Ziegelin, G., Barcena, M., Carazo, J. M., Lurz, R., and Lanka, E. (1997) *J. Biol. Chem. 272*, 30228−36.
36. Stirling, C. J., Szatmari, G., Smith, M. C. M., Steward, G., and Sherratt, D. J. (1988) *EMBO J. 7*, 4389−95.
37. Sunnerhagen, M., Nilges, M., Otting, G., and Carey, J. (1997) *Nature Struct. Biol. 4*, 819−26.
38. Barcena, M., Ruiz, T., Donate, L. E., Brown, S. E., Dixon, N. E., Radermacher, M., and Carazo, J. M. (2001) *EMBO J. 20*, 1462−8.
39. Chen, Y. J., Yu, X., and Egelman, E. H. (2002) *J. Mol. Biol. 319*, 587−91.
40. Patel, S. S., and Picha, K. M. (2000) *Annu. Rev. Biochem. 69*, 651−97.
41. Straume, M., and Johnson, M. L. (1992) *Methods Enzymol. 210*, 87−105.

BI034341B